

ISSN 2072-5981  
doi: 10.26907/mrsej



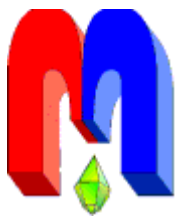
***magnetic  
Resonance  
in Solids***

Electronic Journal

*Volume 21  
Special Issue 4  
Paper No 19403  
1-7 pages  
2019*

doi: 10.26907/mrsej-19403

<http://mrsej.kpfu.ru>  
<http://mrsej.ksu.ru>



Established and published by Kazan University  
Endorsed by International Society of Magnetic Resonance (ISMAR)  
Registered by Russian Federation Committee on Press (#015140),  
August 2, 1996  
First Issue appeared on July 25, 1997

© Kazan Federal University (KFU)\*

*"Magnetic Resonance in Solids. Electronic Journal" (MRSej)* is a peer-reviewed, all electronic journal, publishing articles which meet the highest standards of scientific quality in the field of basic research of a magnetic resonance in solids and related phenomena.

Indexed and abstracted by  
*Web of Science (ESCI, Clarivate Analytics, from 2015), Scopus (Elsevier, from 2012), RusIndexSC (eLibrary, from 2006), Google Scholar, DOAJ, ROAD, CyberLeninka (from 2006), SCImago Journal & Country Rank, etc.*

***Editor-in-Chief***

Boris **Kochelaev** (KFU, Kazan)

***Honorary Editors***

Jean **Jeener** (Universite Libre de Bruxelles, Brussels)


Raymond **Orbach** (University of California, Riverside)

***Executive Editor***

Yurii **Proshin** (KFU, Kazan)  
[mrsej@kpfu.ru](mailto:mrsej@kpfu.ru)



This work is licensed under a [Creative Commons Attribution-ShareAlike 4.0 International License](https://creativecommons.org/licenses/by-sa/4.0/).

 This is an open access journal which means that all content is freely available without charge to the user or his/her institution. This is in accordance with the [BOAI definition of open access](https://www.boai.ru/).

***Special Editor of Issue***

Eduard **Baibekov** (KFU)

***Editors***

Vadim **Atsarkin** (Institute of Radio Engineering and Electronics, Moscow)

Yurij **Bunkov** (CNRS, Grenoble)

Mikhail **Eremin** (KFU, Kazan)

David **Fushman** (University of Maryland, College Park)

Hugo **Keller** (University of Zürich, Zürich)

Yoshio **Kitaoka** (Osaka University, Osaka)

Boris **Malkin** (KFU, Kazan)

Alexander **Shengelaya** (Tbilisi State University, Tbilisi)

Jörg **Sichelschmidt** (Max Planck Institute for Chemical Physics of Solids, Dresden)

Haruhiko **Suzuki** (Kanazawa University, Kanazawa)

Murat **Tagirov** (KFU, Kazan)

Dmitrii **Tayurskii** (KFU, Kazan)

Valentine **Zhikharev** (KNRTU, Kazan)

***Technical Editors of Issue***

Nurbulat **Abishev** (KFU)

Maxim **Avdeev** (KFU)

Eduard **Baibekov** (KFU)

Alexander **Kutuzov** (KFU)

\* In Kazan University the Electron Paramagnetic Resonance (EPR) was discovered by Zavoisky E.K. in 1944.

# Wideband EPR-spectroscopy of $\text{Y}_3\text{Al}_5\text{O}_{12}:\text{Er}^{3+}$ , $(\text{Y}_{0.9}\text{Lu}_{0.1})_3\text{Al}_5\text{O}_{12}:\text{Er}^{3+}$ and $\text{Y}_3\text{Al}_5\text{O}_{12}:\text{Fe}^{2+}$ crystals

H.R. Asatryan<sup>1</sup>, G.S. Shakurov<sup>2,\*</sup>, A.G. Petrosyan<sup>3</sup>, K.L. Hovannesyanyan<sup>3</sup>

<sup>1</sup>Ioffe Physical-Technical Institute of RAS, Politekhnicheskaya 26, St. Petersburg 194021, Russia

<sup>2</sup>Zavoisky Physical-Technical Institute, FRC Kazan Scientific Center of RAS, Sibirsky trakt 10/7, Kazan 420029, Russia

<sup>3</sup>Institute for Physical Research, National Academy of Sciences of Armenia, Ashtarak-2 0203, Armenia

\*E-mail: [shakurov@kfti.knc.ru](mailto:shakurov@kfti.knc.ru)

(Received May 23, 2019; accepted May 28, 2019; published June 6, 2019)

Using an X-band EPR spectrometer and a submillimeter EPR spectrometer,  $\text{Y}_3\text{Al}_5\text{O}_{12}$  (YAG),  $(\text{Y}_{0.9}\text{Lu}_{0.1})_3\text{Al}_5\text{O}_{12}$  (YLuAG) crystals with erbium and YAG with iron were investigated. In YAG:Er crystals the resonance transitions between ground and the first excited doublets in the frequency range 580-750 GHz were observed. The energy interval to the first excited Stark level is measured and the direction of the axes of the  $g$ -tensor of the excited doublet is specified. The field-frequency and angular dependences of these transitions are measured and theoretically calculated. In the YAG:Fe crystal a non-Kramers ion was detected in the frequency range 112-150 GHz. It was concluded that resonant transitions between the  $|+2\rangle \leftrightarrow |-2\rangle$  states of the  $\text{Fe}^{2+}$  ion in the tetrahedral environment are observed.

**PACS:** 71.70.Ej, 76.30.-v, 76.30.Fc, 76.30.Kg.

**Keywords:** multifrequency EPR spectra,  $g$ -factors, zero-field splitting.

*Authors dedicate this manuscript to the 80th jubilee of Professor B.Z. Malkin*

## 1. Introduction

Crystalline compounds with the garnet structure (in particular, yttrium-aluminum garnet  $\text{Y}_3\text{Al}_5\text{O}_{12}$  or YAG) activated by rare-earth ions are among the most used in quantum electronics [1, 2]. At the same time,  $\text{Er}^{3+}$  activated garnets in the past few years have attracted increased interest due to their use as effective active media for lasers of the three-micron range used in medicine. Progress in this area largely depends on the complete knowledge of the spectroscopic properties of these crystals. One of the direct and most informative methods for studying the properties of condensed media is the electron paramagnetic resonance (EPR), which allows identification of the impurity ion, definition of its charge state, local symmetry, and the composition of the nearest environment.

In a cubic garnet crystal (space group  $Ia\bar{3}d$ ), there are three cationic positions that may contain an impurity ion. In YAG, aluminum occupies octahedral positions with a local  $C_{3i}$  symmetry ( $K_\alpha/K_M = 8/8$ ) and tetrahedral positions with a local  $S_4$  symmetry ( $K_\alpha/K_M = 12/6$ ). Yttrium is in a dodecahedron with a local  $D_2$  symmetry ( $K_\alpha/K_M = 12/6$ ). Here,  $K_\alpha$  and  $K_M$  denote crystallographic and magnetic multiplicities, respectively. In YAG crystals  $\text{Er}^{3+}$  ions replace  $\text{Y}^{3+}$  ions. The  $\text{Er}^{3+}$  ion (electron configuration  $4f^{11}$ ) has a ground  $^4I_{15/2}$  multiplet which is splitted by the crystal field into a series of Kramers doublets. A characteristic feature of the compound is the presence of several lower Stark levels with relatively small splittings of 10-100  $\text{cm}^{-1}$ . The scheme of the energy levels of the ground multiplet of the  $\text{Er}^{3+}$  ion in YAG single crystals was studied at helium [3] and room [4] temperatures. It follows from [3] that the energy interval between the ground doublet and the excited one is 22  $\text{cm}^{-1}$ . The next excited doublet has already been removed at 60  $\text{cm}^{-1}$ . In YAG, the EPR of  $\text{Er}^{3+}$  ions in the ground

state were earlier studied in [5]. The splitting between the ground and the first excited doublets made it possible to study the EPR spectra from the thermally populated excited state [6, 7]. Due to the short spin-lattice relaxation times, it is impossible to thermally populate other levels and simultaneously register EPR on them.

Erbium contains an odd isotope  $^{167}\text{Er}$  with the nuclear spin  $I = 7/2$  with a natural abundance of 22.94%. In the X-band, the hyperfine structure (HFS) is observed both in the ground state and the first excited state. The ratio of the intensities of the lines observed in the EPR spectrum corresponds to the natural abundance of erbium isotopes. The following values of the parameter of the  $g$ -tensor were obtained earlier:  $g_x = 3.71 \pm 0.05$ ,  $g_y = 7.75 \pm 0.01$ ,  $g_z = 7.35 \pm 0.05$  for  $\text{Er}_0^{3+}$  (ground state) and  $g_x = 2.036 \pm 0.005$ ,  $g_y = 1.995 \pm 0.001$ ,  $g_z = 14.6 \pm 0.1$  for  $\text{Er}^{13+}$  (excited state) [5, 6]. In this case, for the ground state, the magnetic local axes of  $\text{Er}^{3+}$  ions in YAG are oriented in such a way that the  $z$ -axes are directed along the  $\langle 100 \rangle$  axis of the crystal, and the  $x$  and  $y$ -axes along the  $\langle 110 \rangle$  directions [5]. For the excited state, the EPR spectra were described when the  $z$ -axis was oriented along the  $\langle 110 \rangle$  direction, and  $x$  and  $y$  along the  $\langle 100 \rangle$  and  $\langle 110 \rangle$  directions [6]. Note that in the article [6] it was initially assumed that the spectrum belongs to a new erbium center in a garnet. The belonging of this center to the excited state was established in [7]. In the present work we have carried out high frequency EPR measurements on YAG single crystals doped with trivalent erbium ions. We observed resonant transitions between the ground and the first excited doublet. The purpose of the study was to confirm the available literature data in an independent way and to obtain new spectroscopic information.

Although garnet crystals with iron impurity have been studied previously by the EPR method [8–10], most of the work is devoted to spectroscopy of  $\text{Fe}^{3+}$  ions that enters the octahedral and tetrahedral positions. We know only one work performed by the acoustic paramagnetic resonance (APR) method, in which the non-Kramers state of iron in YAG was observed [11]. The authors attributed the APR spectra to the  $\text{Fe}^{2+}$  ion in the octahedral environment. The ground state of  $\text{Fe}^{2+}$  ion ( $d^6$ ,  $^5D$ ) has a spin  $S = 2$ . Note that although the EPR spectroscopy of  $\text{Fe}^{2+}$  ions is poorly studied, there are literature data on the occurrence of  $\text{Fe}^{2+}$  ions in the position of an oxygen tetrahedron. In particular, in beryl, EPR spectra were previously observed [12], which were attributed to  $\text{Fe}^{2+}$  ions in the oxygen tetrahedron. The main difficulty in identifying the spectra of  $\text{Fe}^{2+}$  is associated with the large fine structure constants. It is convenient to compare  $\text{Fe}^{2+}$  with the well-studied  $\text{Cr}^{2+}$  ion ( $d^4$ ,  $^5D$ ,  $S = 2$ ). In a low-symmetric environment, all the electronic states of divalent chromium are singlets and the wave functions of the states are mixed. Experimental observation of 10 different transitions between spin sublevels immediately removes the question of the magnitude of the spin and the valence state of chromium. In this case, the maximum zero-field splitting (ZFS) values separating the states  $|0\rangle$  and  $|\pm 2\rangle$  are  $\sim 10 \text{ cm}^{-1}$ . In the case of  $\text{Fe}^{2+}$  ions, the maximum ZFS values lie in the terahertz range, which is currently practically not used in the EPR spectroscopy. As a rule, using frequencies up to 1 THz, it is possible to observe only one to three resonant transitions and to describe the EPR spectra by means of the effective spin. This paper essentially describes such case. The EPR spectra of the non-Kramers iron state were observed by us in YAG crystal. From the analysis of the spectra, a conclusion was done about the tetrahedral coordination of  $\text{Fe}^{2+}$  ions. Using a spin Hamiltonian with an effective spin  $S = 1/2$ , the values of the spectral parameters are obtained.

## 2. Details of experiments and results

Single crystals of YAG activated with  $\text{Er}^{3+}$  ions with a concentration of 0.1 at.% and 10 at.% were investigated. Several spectra were also obtained and studied in a mixed  $(\text{Y}_{0.9}\text{Lu}_{0.1})_3\text{Al}_5\text{O}_{12}$

garnet with  $\text{Er}^{3+}$  concentration 0.3 at.%. The crystals were grown by the method of vertical directional crystallization at the Institute for Physical Research of the National Academy of Sciences of Armenia. Details of the growth of crystals with iron impurity were given elsewhere [13].

The spectra were taken at liquid helium temperature with X-band JEOL EPR spectrometer and the high-frequency EPR spectrometer operating in the range of 37-850 GHz ( $1.2\text{-}28\text{ cm}^{-1}$ ) [14] in external magnetic fields up to 9 kG.

The EPR spectra of the YAG:Er crystal were recorded in the frequency range of 37-150 GHz, when observing the intra-doublet resonance transition, and in the range of 580-750 GHz for the inter-doublet transitions. The angular dependence of the EPR spectra for the intra-doublet transition is consistent with the dependence measured in the X-band [5]. The EPR lines of the inter-doublet transitions turned out to be significantly wider than the intra-doublet transitions. In a crystal with an erbium concentration of 0.1%, the widths were  $\sim 6$  GHz and  $\sim 600$  MHz, respectively. This led to the fact that in the inter-doublet transitions, the hyperfine structure was not resolved. View of the EPR spectra of the inter-doublet transitions in the orientation  $\mathbf{B} \parallel \langle 110 \rangle$  is shown in Fig. 1a. In addition to the intense transitions of the ground doublet-excited doublet, additional lines belonging to the new center were observed for both concentrations studied, but because of the low signal to noise ratio their orientation dependencies could not be studied. In the X-band EPR spectra, in addition to the well-known erbium line, a number of satellite lines were also observed. Their angular dependence cannot also be traced due to the spectral overlap, but some of them belong to erbium, which is confirmed by the presence of a hyperfine structure. The angular and field-frequency dependencies of the EPR spectra of the inter-doublet transitions of the main center are shown in Fig. 2 and Fig. 3. It should be noted that in the 630-680 GHz range, the microwave power was too small and measurements were not carried out. Fig. 3 also presents the field-frequency dependence of the new center.

In the YLuAG:Er crystal in the EPR spectra of the intra-doublet transition there was a line with a  $g$ -factor slightly higher than the known value for erbium. Due to the overlapping of the spectra, the angular dependence of the additional line could not be measured, but in some areas where the signals were allowed, we can conclude about a similar angular dependence. An attempt to study in detail the inter-doublet transitions in a single crystal  $(\text{Y}_{0.9}\text{Lu}_{0.1})_3\text{Al}_5\text{O}_{12}$  was unsuccessful due to the small signal to noise ratio and too large widths of EPR lines (Fig. 1b).

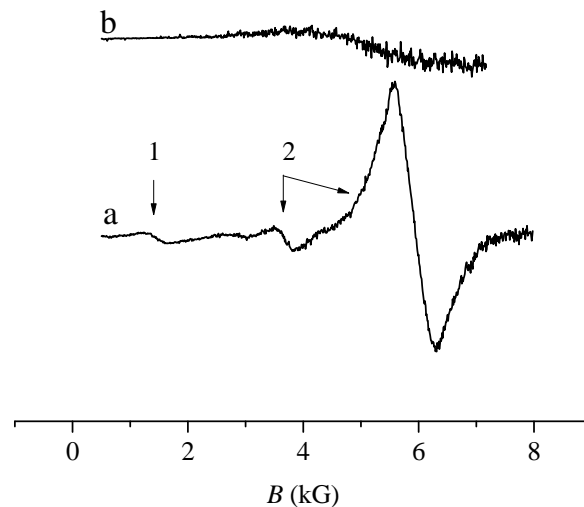


**Figure 1.** EPR spectra in crystals: (a) YAG:Er $^{3+}$  (0.1%),  $\nu = 611.5$  GHz,  $\mathbf{B} \parallel \langle 110 \rangle$ , 1 – new center, 2 – known center; (b) YLuAG:Er $^{3+}$ ,  $\nu = 612$  GHz.

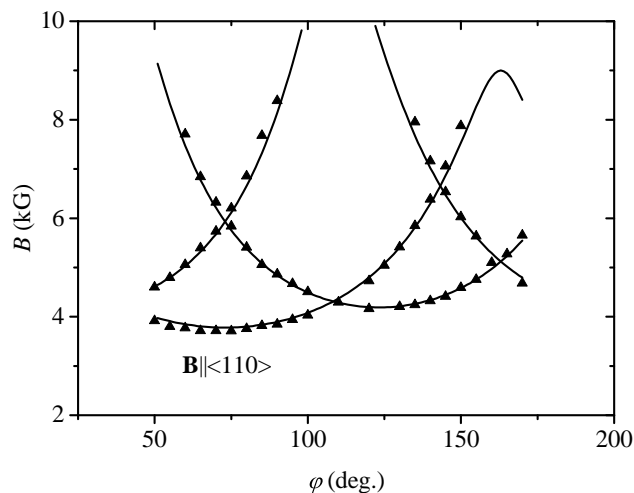


**Figure 2.** Measured (symbols) and calculated (solid line) angular dependence of the EPR spectra in  $\text{YAG}:\text{Er}^{3+}$  crystal at the frequency 611 GHz. Rotation in crystallographic plane  $\{110\}$ .

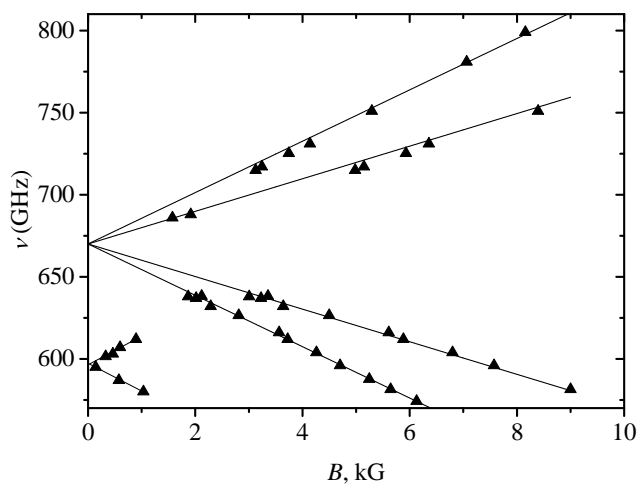


**Figure 3.** Measured (symbols) and calculated (solid lines) field-frequency dependence of the EPR spectra in  $\text{YAG}:\text{Er}^{3+}$  crystal.  $\mathbf{B} \parallel \langle 110 \rangle$ .

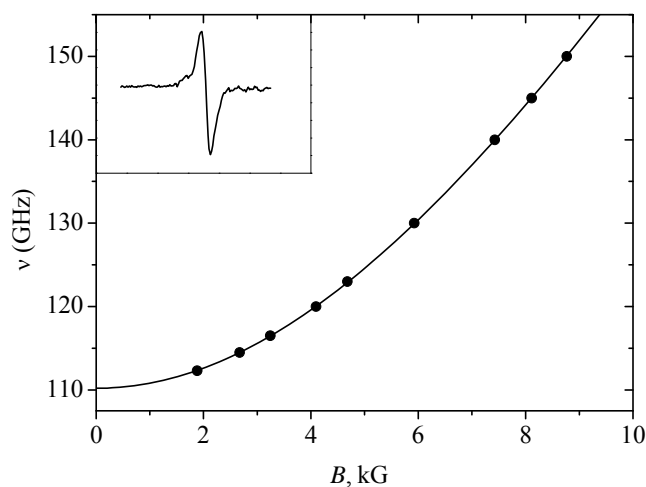


**Figure 4.** Measured (symbols) and calculated (solid line) field-frequency dependence of the EPR spectra in a  $\text{YAG}:\text{Fe}^{2+}$  crystal.  $\mathbf{B} \parallel \langle 100 \rangle$ . The inset shows the EPR spectrum at 115.2 GHz.

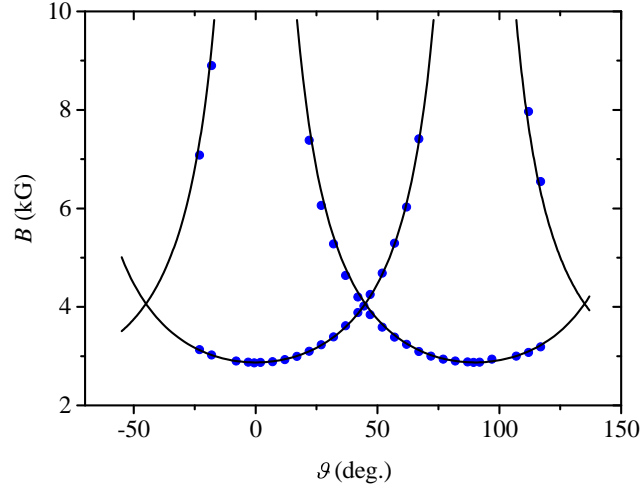


**Figure 5.** Measured (symbols) and calculated (solid line) angular dependence of the EPR spectra in a YAG:Fe<sup>2+</sup> crystal at the frequency 115.2 GHz. Rotation in crystallographic plane {100}.

In the YAG:Fe crystal, resonant transitions were found in the frequency range of 112-150 GHz. The EPR lines were observed at collinear polarization of microwave magnetic field ( $\mathbf{B}_0 \parallel \mathbf{B}_1$ ). Fig. 4 shows the EPR spectrum and the field-frequency dependence of the resonant transitions for the orientation  $\mathbf{B} \parallel (100)$ . The absence of a conjugate branch in this dependence indicates a transition to the singlet-singlet type. The angular dependence of the EPR spectra is shown in Fig. 5. The direction of the  $z$ -axis (along the fourth-order axis) and the number of magnetically nonequivalent centers (6) allow us to conclude that the impurity is localized in the oxygen tetrahedron (local symmetry  $S_4$ ). As in the case of erbium impurity, weak satellite signals were observed in the spectra near the main lines, which were not studied due to the small signal to noise ratio.

### 3. Discussion

The calculation of the angular dependences of the inter-doublet transition was made by numerical diagonalization of the fourth-order energy matrix, the elements of which were calculated using the following Hamiltonian:

$$H = g_J \mu_B \mathbf{B} \mathbf{J} + \Delta_{ij}$$

where the first term is the Zeeman energy, and the second takes into account the ZFS between two doublets ( $\Delta_{ij} = 0$  if  $i \neq j$ ). For the matrix elements of the Zeeman interaction, we used the experimental values of  $g$ -factors of the main and first excited doublets [5, 6] and the only variable parameter was the value of ZFS. The results presented in [6] describe the experimental angular dependence of the EPR spectra measured in the X-band for an excited doublet, but they were obtained without taking into account the values of the  $g$ -tensor of the ground doublet. Since the directions of the magnetic axes in [5–7] did not match for the ground and excited doublets, it was necessary to bring them to a single system. When calculating the angular dependence of the inter-doublet transitions, agreement between the experiment and the theory occurs for the following axial directions:  $g_x = 3.71$ ,  $g_y = 7.75$ ,  $g_z = 7.35$  Er<sub>0</sub><sup>3+</sup> (ground state) and  $g_x = 1.995$ ,  $g_y = 14.6$ ,  $g_z = 2.036$  for Er<sub>1</sub><sup>3+</sup> (excited state). After the fitting we got the value ZFS = 670 GHz. In Fig. 2 the result of the calculation is presented by a solid line. Taking into account the measurement error of the frequency ( $\pm 0.5$  GHz), the calculated curves satisfactorily describe the experimental data and confirm that the observed angular dependence is indeed due to resonant transitions between the main and first excited doublet. Using the obtained spectral

parameters, we also constructed the computed field-frequency dependencies of the inter-doublet transition (Fig. 3) for the two most intense magnetically-nonequivalent centers. The same Fig. 3 shows the dependence of the additional transition with the magnitude of the ZFS, measured by the direct method, which is equal to  $595 \pm 0.5$  GHz. In this case, solid lines are drawn to trace their behavior in a magnetic field. The presence of a center with such a ZFS in YAG crystals with two different concentrations of the impurity erbium ion indicates that it also belongs to erbium. Thus, the presence of additional erbium centers in YAG crystals has been established.

The mechanisms of formation of additional centers in the YAG crystal are explained by the presence of so-called “antisite” defects (AD). Centers of this type were studied in detail in [15]. In this case, a rare-earth ion replaces yttrium, but the nearest medium is distorted by the presence of a defect. Since we have isovalent replacement, it is obvious that these defects cannot be related to local charge compensation. In the YAG crystals such violations may occur due to uncharacteristic (non-equivalent) substitutions  $\text{Y}^{3+} \rightarrow \text{Al}^{3+}$  in the octahedral nodes, or  $\text{Al}^{3+} \rightarrow \text{Y}^{3+}$  in the dodecahedral nodes. The number of such defects is possible within 4-6% in the process of growing single crystals from the melt. In a mixed garnet, irregular replacement of yttrium by lutetium leads to such a large broadening of the EPR line of the inter-doublet transition (Fig. 1b), that it is impossible to register the AD.

Our assumption that the center observed in YAG:Fe belongs to the  $\text{Fe}^{2+}$  ion is based on the following facts. The presence of iron impurities in the crystal is confirmed by the intense EPR spectra of the  $\text{Fe}^{3+}$  ion, which are recorded in the X-band [13]. The non-Kramers state of a paramagnetic ion localized in a tetrahedron is indicated by the field-frequency and angular dependencies of the spectra. Collinear polarization ( $\mathbf{B}_0 \parallel \mathbf{B}_1$ ) in observing the EPR spectra indicates the selection rules  $\Delta m_S = 0$ . In the splitting of a non-Kramers doublet (for example,  $|\pm 2\rangle$ ), the wave functions of the states of the doublet are mixed and such resonant transitions are observed. The description of the experimental data was obtained using the spin Hamiltonian

$$H = g\mu_B B_z J_z + \Delta S_x$$

with effective spin  $S = 1/2$ , where  $\Delta$  is the ZFS value. By the least squares method, the following spectral parameters were obtained for the field-frequency dependence:  $g = 8.3 \pm 0.1$ ,  $\Delta = 110.2 \pm 0.5$  GHz. Assuming that the observed EPR lines are caused by resonant transitions between the  $|+2\rangle$  and  $|-2\rangle$  states of non-Kramers doublet, we obtain the  $g$ -factor  $g \approx 2.1$ , which is consistent with the values characteristic for  $\text{Fe}^{2+}$  ions. In Fig. 4 and Fig. 5, the solid lines show the calculated curves constructed using the obtained parameters. The angular dependencies are approximated by the function  $1/\cos \alpha$ . Note, the possible valence state of iron, which has  $S = 2$ , is also the  $\text{Fe}^{4+}$  state ( $d^4$ ,  ${}^5D$ ), however, the formation of such a charge state seems unlikely to us.  $\text{Fe}^{4+}$  ions are usually formed in crystals after their exposure to radiation. In addition, for the  $d^4$  configuration, we should expect the value of the  $g$ -factor less than two.

#### 4. Summary

In garnet crystals with erbium impurities, we clarified the position of the first excited level, corrected the orientation of the  $g$ -tensor axes, and measured the energy interval between the main and first excited doublet of the “antisite” defect. In the YAG:Fe crystal the EPR spectrum from the  $\text{Fe}^{2+}$  ion is registered in a tetrahedral environment. Its spectral parameters are determined.

#### Acknowledgments

The authors are grateful to V.A. Shustov for X-ray diffraction measurements and orientation of the samples.



## References

1. Kaminskii A.A. *Laser Crystals*, Nauka, Moscow (1975) (*in Russian*)
2. Kaminskii A.A., Antipenko B.M. *Multilevel Functional Crystal Laser System*, Nauka, Moscow (1989) (*in Russian*)
3. Gruber J.B., Quagliano J.R., Reid M.F., Richardson F.S., Hills M.E., Seltzer M.D., Stevens S.B., Morrison C.A., Allik T.H. *Phys. Rev. B* **48**, 15561 (1993)
4. Agladze N.I., Balashov A.A., Zhizhin G.N., Popova M.N. *Optica i spektroskopiya* **57**, 379 (1984) (*in Russian*)
5. Bull M., Garton G., Leask M.J.M., Ryan D., Wolf W.P. *J. Appl. Phys. Suppl.* **32**, 267S (1961)
6. Baranov P.G., Jekov V.I., Murina T.M., Prokhorov A.M., Khramtsov V.A. *Phys. Solid State* **29**, 723 (1987) [*Fizika Tverdogo Tela* **29**, 1261 (1987)]
7. Asatryan H.R., Baranov P.G., Jekov V.I., Murina T.M., Prokhorov A.M., Khramtsov V.A. *Phys. Solid State* **33**, 559 (1991) [*Fizika Tverdogo Tela* **33**, 976 (1991)]
8. Geshwind S. *Phys. Rev.* **121**, 363 (1961)
9. Rimai L., Kushida T. *Phys. Rev.* **143** 160 (1966)
10. Chen C.Y., Pogatshnik G.J., Chen Y., Kokta M.R. *Phys. Rev. B* **38**, 8555 (1988)
11. Akhmadullin I., Golenishev-Kutuzov V., Migachev S., Korzhik M. *J. Phys. Chem. Solids* **54**, 117 (1993)
12. Shakurov G.S., Khaibullin R.I., Thomas V.G., Fursenko D.A., Mashkovtsev R.I., Lopatin O.N., Nikolaev A.G., Gorshunov B.P., Zhukova E.S. *Phys. Solid State* **59**, 1600 (2017)
13. Shakurov G.S., Asatryan H.R., Mingalieva L.V., Petrosyan A.G., Hovhannesian K.L. *Phys. Solid State* **60**, 2046 (2018)
14. Tarasov V.F., Shakurov G.S. *Appl. Magn. Reson.* **2**, 571 (1991)
15. Asatryan G.R., Kramushchenko D.D., Uspenskaya Yu.A., Baranov P.G., Petrosyan A.G. *Phys. Solid State* **56**, 1150 (2014)